Pion production cross sections and analyzing powers in the inclusive $^{12}C(p,\pi^+)X$ reaction at 400 and 450 MeV

W. R. Falk
Physics Department, University of Manitoba, Winnipeg, Manitoba, Canada

E. G. Auld, G. Giles, G. Jones, G. J. Lolos,* and W. Ziegler
Physics Department, University of British Columbia, Vancouver, British Columbia, Canada

P. L. Walden
TRIUMF, Vancouver, British Columbia, Canada
(Received 1 August 1985)

Inclusive differential cross sections and analyzing powers of the (p,π^+) reaction on ^{12}C have been obtained at 400 and 450 MeV incident proton energies. The energy domain investigated spans the region of pion energies that arise in the $pp\rightarrow d\pi^+$ reaction, a reaction which was measured at the same time. A 65 cm Browne-Buechner spectrometer, in a single-arm configuration, was used for detecting the pions. Measurements were made in the angular range of 46°–88° (lab). At forward angles the measured analyzing powers in the $^{12}C(p,\pi^+)X$ reaction are quantitively similar to those of the $pp\rightarrow d\pi^+$ and $pp\rightarrow pn\pi^+$ reactions, but at backward angles they are considerably more negative. The analyzing power data for angles $\lesssim 70°$ (lab) are consistent with the predictions of a simple quasi-free model that incorporates the free $pN\rightarrow NN\pi^+$ data. Moreover, this model makes a reasonable prediction of the overall strength of the differential cross sections and also reproduces the qualitative shape of the pion energy distributions.

I. INTRODUCTION

It is rather surprising, considering that meson factories at TRIUMF, SIN, and LAMPF have now been in operation for about a decade, to find so little data in the published literature on continuum pion production differential cross sections, especially at energies lower than 500 MeV. Optimization of secondary pion channels clearly relies on the availability of such data. Even more scarce, not unexpectedly, are analyzing power data using polarized beams. Much of the data that do exist were obtained from measurements made well before the meson factories came into existence, and many of these data are available only in unpublished reports. An extensive survey of the literature on pion production on nuclei has been given by Crawford *et al.*[1] This paper[1] also presents a comprehensive set of new data on π^+ and π^- production at 585 MeV, on a wide range of nuclei, data that includes angular distributions of analyzing powers as well as differential cross sections. Recent inclusive measurements on several different targets have been carried out at 180 and 201 MeV proton bombarding energy by Bimbot *et al.*[2] Bridging the gap between these lower energy measurements and those at 585 MeV are the recently reported results by DiGiacomo *et al.*[3] of inclusive $\pi^\pm$ cross sections on ^{12}C and ^{238}U at 330, 400, and 500 MeV. They report only their angle integrated inclusive momentum distributions, and no analyzing power results are available from either these latter experiments or those of Bimbot *et al.*[2] Other measurements pertinent to the present investigation have been made by Mathie.[4]

Inclusive pion production data are of no small importance in the testing of, and further development of, theoretical models[5,6] of pion production. Nucleon-nucleon interactions form the primary starting point of all theoretical descriptions of pion production on nuclei. The isobar model of Sternheim and Silbar[6] assumes the intermediate formation of the $\Delta(1232$ MeV), from which follows the relative strengths of all the $NN\rightarrow NN\pi$ pion production channels. Thus this model should be most appropriate at nucleon bombarding energies of 500–700 MeV, near the peak of the resonance in free nucleon-nucleon collisions. Their model, applied to 730 MeV on a number of nuclei, achieved a considerable measure of success including the correct prediction of the observed π^+ to π^- total production cross section ratio and the dependence of this production cross section on the nuclear size. The pion energy distributions at fixed angle as well as the angular dependence were quite well reproduced for positive pions. A model that retains as a basic ingredient the intermediate formation of the Δ resonance, but incorporates many refinements to account for dynamical and nuclear effects, is the intranuclear cascade model (INC).[7] Only recently[3] has this model been subjected to testing in $A(p,\pi)X$ reactions at bombarding energies below 500 MeV. Overall, rather satisfactory agreement between the predictions of this model and the experimental data is obtained for the angle integrated inclusive momentum distributions. Nevertheless, from the calculations presented in the present paper we are able to conclude that the effective NN center of mass (c.m.) energy that dominates the continuum cross sections at 450 MeV proton bombarding

energy is ~2120 MeV, or about 50 MeV below the NΔ peak energy. Consequently, the $pp \rightarrow d\pi^+$ two-body final state reaction will be proportionately much more important, and this reaction is not adequately described by these models. Finally, no polarization observables are calculated in the INC model in its present formulation. For the data presented in this paper comparisons are made with the predictions of a very simple model that assumes the quasifree production of pions from the nucleons in the nuclear target via the primary $pp \rightarrow d\pi^+$ and $pN \rightarrow NN\pi^+$ reactions. Analyzing powers as well as differential cross sections are calculated in this model.

II. EXPERIMENTAL PROCEDURE

A. Detection efficiency and spectrometer solid angle

The data presented in this paper were recorded during detailed $pp \rightarrow d\pi^+$ calibration measurements of a 65 cm Browne-Buechner magnetic spectrometer used for a program of nuclear pion production measurements at TRIUMF. These calibration measurements were performed using a CH_2 target from which a subtraction of the background from the carbon pions was required. Each measurement on the CH_2 target (areal density: 149 mg/cm^2) was followed by a measurement on a carbon target (areal density: 162 mg/cm^2) under identical beam and spectrometer conditions.

The spectrometer system, shown in Fig. 1, incorporated three helically wound multiwire proportional chambers (MWPC's) for the track reconstruction needed for pion momentum definition. A fast threefold coincidence of scintillation counters (CE $C1$ $C2$) was used for definition of the event trigger. Identification of the pion events was made on the basis of energy loss, time of flight, and track reconstruction. The performance of this system has been described in detail by Ziegler.[8] The line shape of a monoenergetic group of input pions was determined using pions from the $pp \rightarrow d\pi^+$ reaction measured in coincidence with the associated deuteron. For the carbon measurements, the pions of interest for this paper (with energies in the range of 20–140 MeV) were part of a more extensive spectrum extending to much higher energy. These more energetic and copious pions could multiply scatter from the magnet pole faces and subsequently be interpreted as lower energy pions. This phenomenon was exacerbated by the lack of axial focusing in the spectrometer.

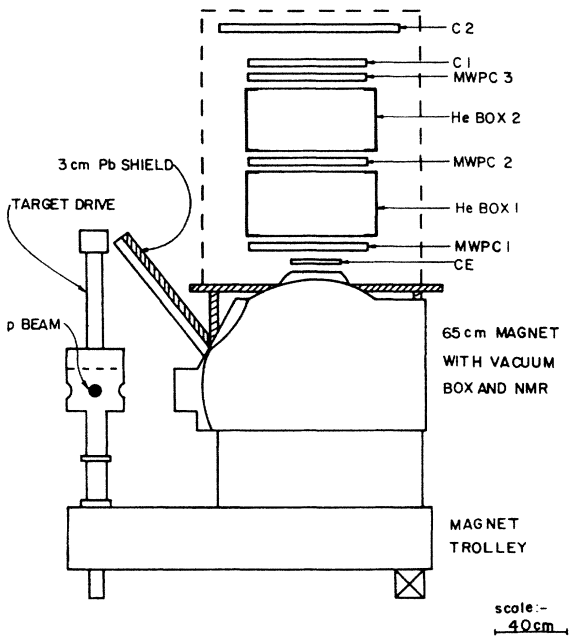

FIG. 1. Pion spectrometer system.

The multiply scattered events were distinguished from the other "good" events by measuring the different survival rates of these two types of events when various software cuts were applied to the data. Typically, the fraction of the multiply scattered events which survived the software cuts was about 0.15, compared to about 0.63 for the good events. Defining these two probabilities as ξ and α, respectively (for a given region of the momentum plane), and β as the combined efficiency for both components, we find

$$\beta=(\alpha Y+\xi b)/(Y+b) , \tag{1}$$

where Y and b are the number of good and scattered events in this region, respectively, before the cuts are applied. The final number of events in the region with cuts applied is

$$N=\alpha Y+\xi b , \tag{2}$$

which, on eliminating b, yields

$$Y=N(\beta-\xi)/[\beta(\alpha-\xi)] . \tag{3}$$

β and N were measured directly for each region of the focal plane; α was determined from a measurement of the survival probability in the peak region of the $pp \rightarrow d\pi^+$ reaction, recorded with a CH_2 target from which the carbon background had been subtracted. Coincidence measurements between the pion and the deuteron from the $pp \rightarrow d\pi^+$ reaction were performed in a separate experiment[8] and indicated that in the extended "tails" on either side of the peak, consisting of events arising from multiple scattering, the fraction of the events surviving the software cuts was about 0.15. This was the value used for ξ, which was also assumed to be the appropriate survival probability for the more energetic multiply scattered pions from carbon recorded in the detection system. Fortunately, the exact value of this parameter is not particularly critical as far as the magnitude of the calculated cross sections is concerned; the shape of the energy distributions is even less affected.

A parametrization of α and β was carried out as a function of focal plane position and magnetic field setting over the full range of values associated with the measurements reported in this paper. Typical values of these parameters for one particular measurement are given in Table I. The results in this table reflect values of b/Y ranging from 24% at the highest pion energies to 31% at the lowest pion energies. These values depend primarily

TABLE I. Details for one particular measurement for $T_p=400$ MeV, $\theta_{lab}=56°$, and $B=6.929$ kG.

T_π interval (MeV)	N[a]	β	α	Y/N[b]	$\Delta\Omega_{eff}$ (msr)	$d^2\sigma/d\Omega\,dT_\pi$ (μb/sr MeV)	A_N
45.5–47.8	927±18	0.509	0.621	1.499	1.86	7.56±0.15	−0.239±0.037
47.8–49.9	1019±19	0.519	0.637	1.461	1.94	8.14±0.15	−0.346±0.034
49.9–52.0	1022±19	0.530	0.653	1.426	1.99	8.15±0.15	−0.344±0.034
52.0–54.0	1049±19	0.540	0.666	1.399	2.03	8.41±0.16	−0.371±0.034
54.0–55.9	1039±19	0.551	0.678	1.378	2.05	8.46±0.16	−0.346±0.034
55.9–57.7	1021±19	0.562	0.688	1.362	2.05	8.54±0.16	−0.344±0.034
57.7–59.5	1012±19	0.572	0.696	1.350	2.06	8.72±0.16	−0.342±0.035
59.5–61.1	994±19	0.583	0.703	1.344	2.06	8.85±0.17	−0.325±0.035
61.1–62.8	935±18	0.593	0.707	1.341	2.06	8.65±0.17	−0.380±0.036
62.8–64.3	928±18	0.604	0.711	1.339	2.04	8.97±0.18	−0.251±0.037

[a] The number of events in the interval has been normalized to a given proton flux and corrected for the wire chamber efficiency.
[b] $Y/N=(\beta-\xi)/[\beta(\alpha-\xi)]$, with $\xi=0.15$.

on the pion energy and exhibit little angular dependence. Statistical uncertainties in the determination of α and β were about 1% and 3%, respectively.

The effective solid angle of the spectrometer was determined from the measured yields for the $pp\rightarrow d\pi^+$ reaction, corrected for software cuts and wire chamber efficiencies. The effective solid angle representing the product of the geometrical solid angle multiplied by the pion survival probability, measured at the center of the focal plane, varied from about 2.2 msr at 100 MeV to 1.6 msr at 30 MeV pion energy. Relative uncertainties in these values are ±5%, with absolute uncertainties of ±10%. Dependence of the solid angle on focal plane position was mapped by moving the $pp\rightarrow d\pi^+$ peak over the range of acceptance of the spectrometer. Cross section input data required for this calibration were taken from Richard-Serre *et al.*[9] (350–500 MeV), and Jones[10] at 400 MeV, and from the parametrization of Ver West and Arndt[11] at 450 MeV. The values used are in good agreement with the more recently measured values of Giles *et al.*[12] The angular dependence was determined from parameters given in Ref. 10.

B. Beam normalization and polarization

Simultaneous measurement of the polarization and intensity of the proton beam was accomplished using elastic p-p scattering from a CH_2 target in a four-arm eight-counter polarimeter[4,13] that detected both the scattered and recoil protons. The analyzing power of the polarimeter was 0.34 and 0.35 at 400 and 450 MeV, respectively. Typical beam polarizations were 66% with intensities 1–2 nA.

C. Calculation of cross sections and analyzing powers

The yield Y, corrected for the software cuts and wire chamber efficiencies as described in Sec. II A above, is related to the double differential cross section by the expression

$$Y=n_p n_t \Delta T_\pi \Delta\Omega_{eff}(d^2\sigma/d\Omega\,dT_\pi)\,, \tag{4}$$

where n_p is the number of incident protons, n_t the number of target nuclei per cm^2, ΔT_π the energy interval, and $\Delta\Omega_{eff}$ the effective spectrometer solid angle defined in Sec. II A, corrected for focal plane position. Denoting for the moment the double differential cross section for spin up and spin down (defined according to the Madison convention[14]) by σ^+ and σ^-, respectively, the spin averaged cross section is then

$$d^2\sigma(\theta,T_\pi)/d\Omega\,dT_\pi=\frac{P^-\sigma^+ + P^+\sigma^-}{P^- + P^+}\,, \tag{5}$$

where P^+ and P^- are the beam polarizations for spin up and spin down, respectively. The analyzing power is given by

$$A_N(\theta,T_\pi)=\frac{\sigma^+ - \sigma^-}{P^+\sigma^- + P^-\sigma^+}\,. \tag{6}$$

Numerous measurements, corresponding to different magnetic field settings for the spectrometer, were made at each angle for each of the beam energies of 400 and 450 MeV. Cross sections and analyzing powers for a single typical measurement are presented in Table I. Final cross

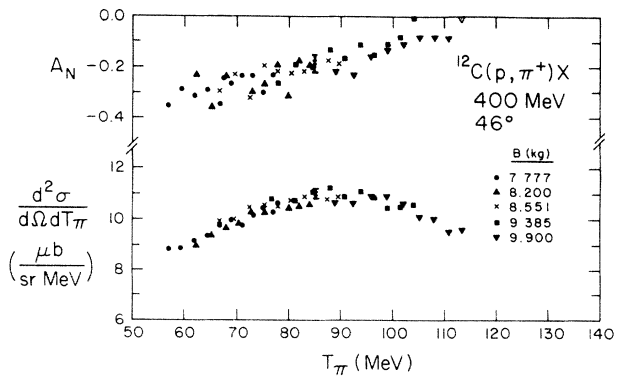

FIG. 2. Cross sections and analyzing powers of the $^{12}C(p,\pi^+)X$ reaction at 400 MeV and 46°, comparing individual measurements at different magnetic field settings. All quantities are given in the laboratory frame. Typical error bars are indicated.

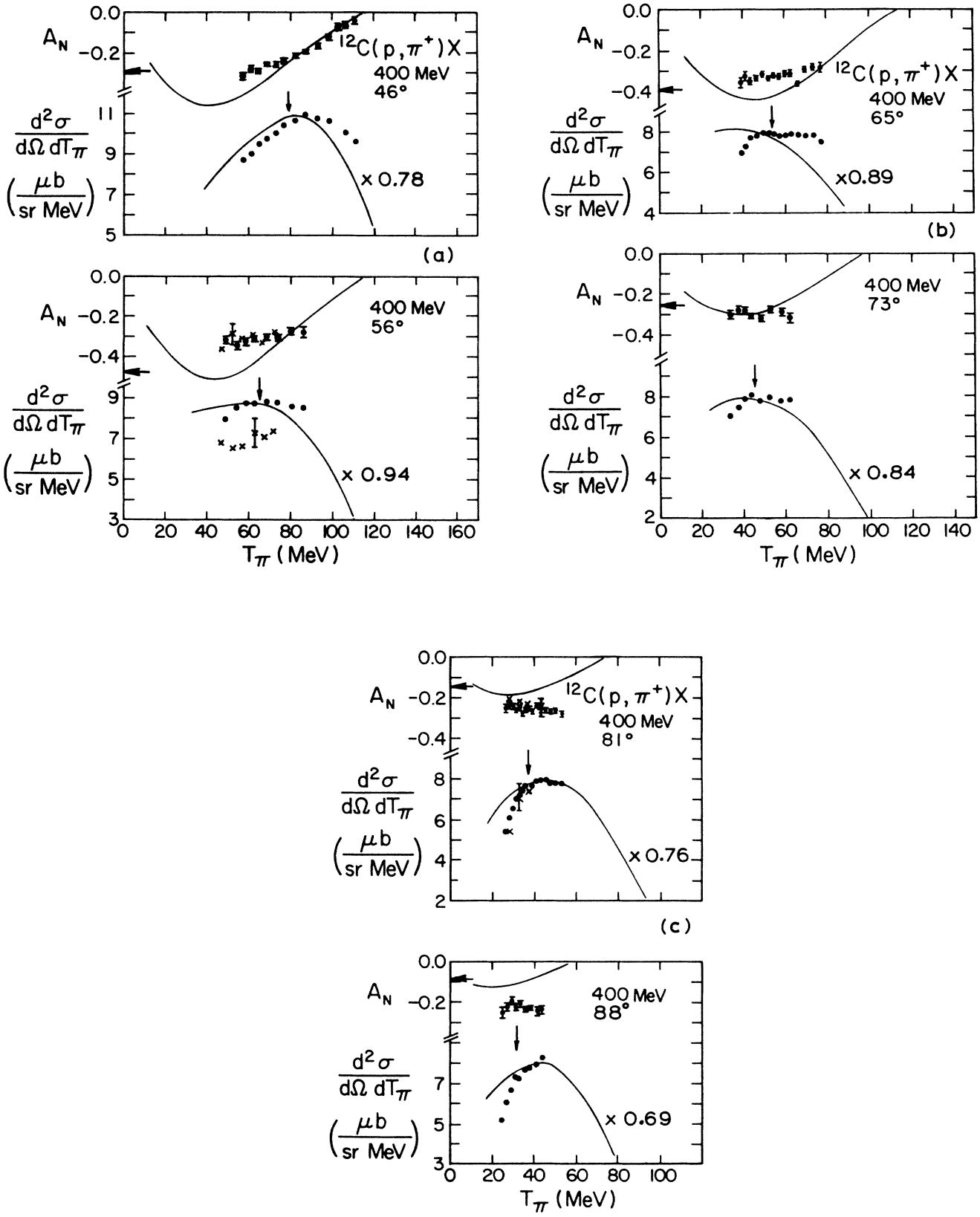

FIG. 3. Cross sections and analyzing powers of the $^{12}C(p,\pi^+)X$ reaction at 400 MeV as a function of the pion kinetic energy. All quantities are given in the laboratory frame. The full circles are from the present measurements and the crosses from Ref. 4. The solid curves are the predictions of the model as described in the text. These calculated cross sections were multiplied by the factor indicated on each curve, prior to plotting.

sections and analyzing powers represent averages of data points taken from measurements of overlapping momentum ranges. Comparison of individual measurements at different field settings confirmed the internal consistency of the various calibrations and cut efficiencies, as shown in Fig. 2. The results shown in the subsequent figures have been averaged over energy intervals varying from about 2 MeV at the lowest pion energies to 5 MeV at the highest pion energies.

III. EXPERIMENTAL RESULTS

Results for the cross sections and analyzing powers[15] are summarized in Figs. 3 and 4 for 400 and 450 MeV, respectively. The error bars on the analyzing powers represent the statistical uncertainties only; the corresponding errors in the cross sections are not shown but were typically about 1%. The overall normalization uncertainty in the cross sections is estimated at 10%. A further relative uncertainty of 10% applies between different sets of measurements due to uncertainties in the effective solid angle and the cut efficiencies. Previous measurements at 400 MeV on carbon, over a somewhat more restricted pion energy range, have been performed by Mathie.[4] There is good agreement overall in the analyzing power measurements from these two completely independent experiments. The differential cross sections of Mathie,[4] are approximately 20% smaller at forward angles, very similar at 81°, and about 10% greater at 88°. This agreement must be considered very satisfactory given the fact that Mathie's data were not corrected for multiple scattering. Some of Mathie's data[4] are shown in Figs. 3(a) and (c) for comparison.

Also indicated in Figs. 3 and 4 (vertical arrows) are the pion energies for the $pp \rightarrow d\pi^+$ reaction at the corresponding angles. The differential cross sections generally exhibit a broad maximum in the neighborhood of this two-body energy. The horizontal arrows in the figures indicate the analyzing powers[16] of the $pp \rightarrow d\pi^+$ reaction at the corresponding angles and bombarding energies. For these in-

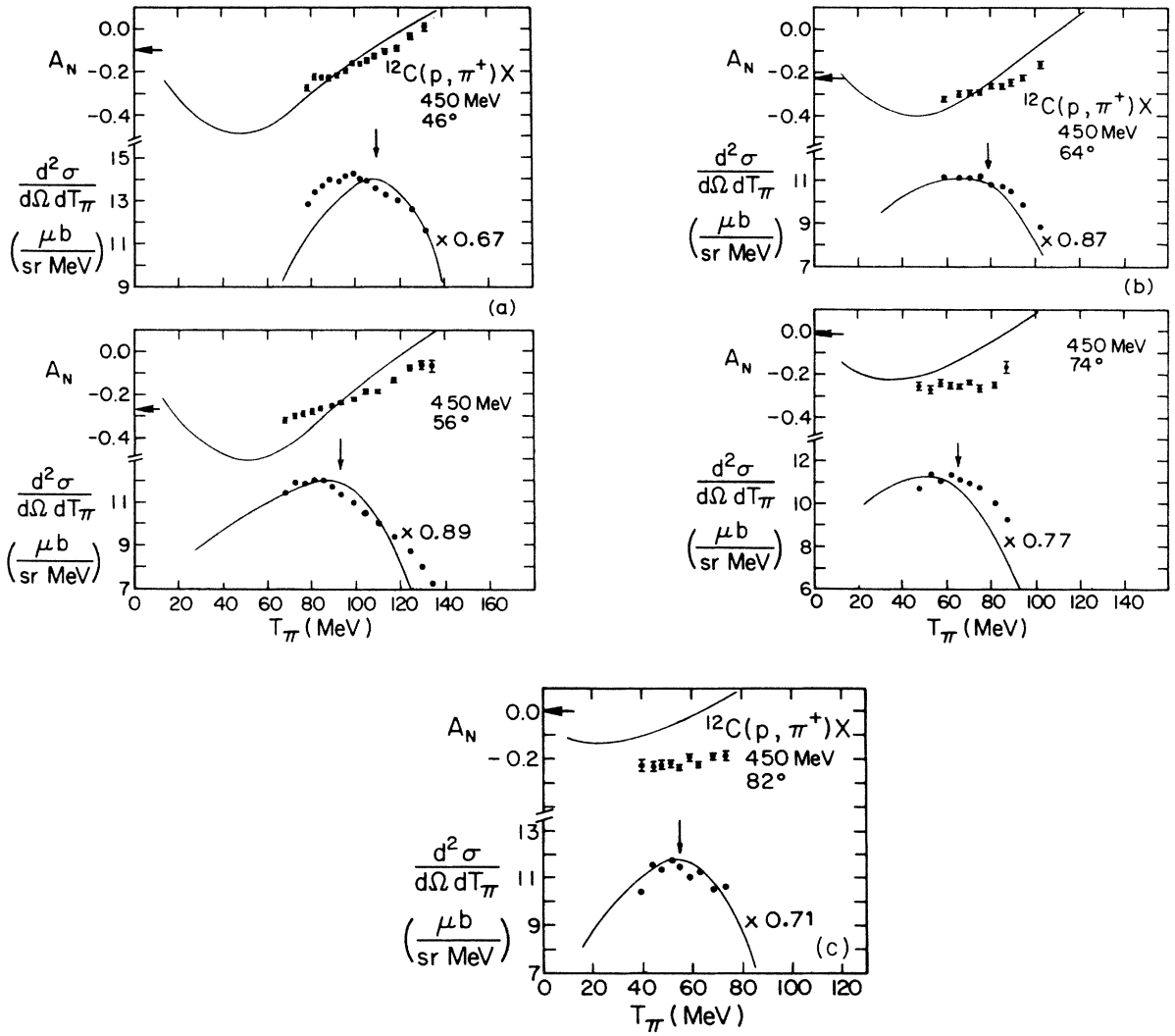

FIG. 4. Cross sections and analyzing powers of the $^{12}C(p,\pi^+)X$ reaction at 450 MeV. Other details as in Fig. 3.

clusive measurements on carbon very significant values of the analyzing powers are observed at all angles, with an angular dependence much less pronounced than in the free $pp \rightarrow d\pi^+$ reaction. Moreover, at the larger angles they are considerably more negative than for the $pp \rightarrow d\pi^+$ case. A strong dependence of the analyzing power on the pion energy is observed at the most forward angle of 46° at both 400 and 450 MeV bombarding energy. These qualitative characteristics of both the cross section and analyzing power energy distributions are strongly suggestive of a quasifree origin of the pions in this kinematical regime, with broadening of the distributions due to the effects of the Fermi motion of the struck nucleons. The curves shown in Figs. 3 and 4 are the predictions of such a quasifree model which is discussed in more detail in the following section.

IV. INCLUSIVE PION PRODUCTION IN A QUASIFREE MODEL

Since many of the observational features of the inclusive pion production results appear similar to those of the free $pp \rightarrow d\pi^+$ reaction at the same kinematical values, we have investigated the extent to which a simple model based on the elementary $pp \rightarrow d\pi^+$ and $pN \rightarrow NN\pi^+$ pion production processes is able to describe the observations. Cross sections for the three π^+ production reactions are expressed below in terms of the initial and final nucleon isospin states, according to Ver West and Arndt.[11]

$$pp \rightarrow d\pi^+, \ \sigma_{10}^{d} ,$$

$$pp \rightarrow pn\pi^+, \ \sigma_{10}+\sigma_{11} ,$$

$$pn \rightarrow nn\pi^+, \ \tfrac{1}{2}(\sigma_{11}+\sigma_{01}) .$$

The first reaction has the higest cross section near threshold; however, at 480 MeV bombarding energy the total $pp \rightarrow pn\pi^+$ reaction cross section is already equal to the $pp \rightarrow d\pi^+$ total reaction cross section[11] and rises much more rapidly with increasing energy thereafter. Furthermore, σ_{11} is much less than σ_{10} near threshold but rises to about 25% of σ_{10} at 500 MeV bombarding energy. Perhaps the dominance of this $1 \rightarrow 0$ isospin transition in the $pp \rightarrow pn\pi^+$ reaction below 500 MeV explains why the analyzing powers for this reaction can be well described[17] with a simple calculation using the $pp \rightarrow d\pi^+$ analyzing power data as input.

The present calculation uses as input the total cross sections for $NN \rightarrow NN\pi^+$ production as given by Ver West and Arndt,[11] but assumes the angular and spin dependence for the unbound NN final system to be the same as that for the $pp \rightarrow d\pi^+$ reaction. Since the interest was not in a detailed quantitative comparison at this stage, we have completely neglected such potentially important effects as distortion in the incident and outgoing channels, nuclear structure effects, and pion charge exchange. However, the Fermi motion of the struck nucleons, required in order to understand the energy dependence in the data, will play an increasingly important role as the bombarding energy approaches the threshold for pion production in free NN collisions. This effect has thus been included in the model. Momentum distributions of protons in ^{12}C as measured in (e,e'p) experiments[18] were used.

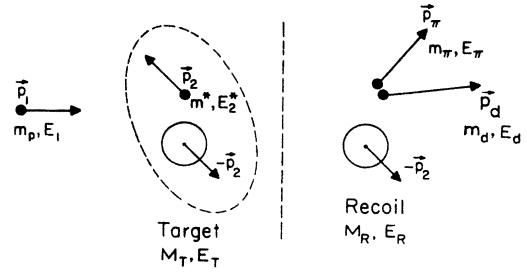

FIG. 5. Model of the quasifree pion production mechanism in nuclei.

We assume the interaction of the incident proton with an off-shell proton (or neutron) of the target nucleus as illustrated in Fig. 5. It is assumed that a final state results consisting of a pion, a deuteron (or unbound NN system), and the recoil nucleus. Overall energy conservation then yields

$$E_1+E_T=E_\pi+E_d+E_R , \tag{7}$$

where these quantities refer to the total energies of the incident proton, the target nucleus, the pion, the deuteron (or NN system), and the recoil nucleus, respectively. The off-shell proton of the target nucleus has a total energy E_2^*; thus the "two-body" reaction, in which the rest of the nucleons participate only as "spectators," satisfies the condition

$$E_1+E_2^*=E_\pi+E_d , \tag{8}$$

from which we obtain

$$E_2^*=E_T-E_R . \tag{9}$$

The recoil nucleus is considered to be on shell and has a kinetic energy (nonrelativistic) of $p_2^2/2M_R$, where p_2 is the momentum of the struck proton. In terms of the separation energy E_s of a proton from ^{12}C, defined as

$$E_s=[(M_R+m_p)-M_T]c^2 , \tag{10}$$

the total energy of the struck proton is then

$$E_2^*=m_pc^2-E_s-p_2^2/2M_R . \tag{11}$$

The rest mass energies of the target, the proton, and the recoil nucleus (to the state in question) are, respectively, M_Tc^2, m_pc^2, and M_Rc^2. The mean separation energies for the p- and s-shell protons (to all final states) measured in electron scattering are 17.5 and 38.1 MeV, respectively,[18] whereas the proton separation energy to the ground state of ^{11}B is 15.96 MeV.

Complete kinematic calculations were carried out for the collision of an incident proton with a target nucleon having energies E_1 and E_2^* and momenta $\mathbf{p}_1$ and $\mathbf{p}_2$, respectively. The projection of the incident proton spin on the axis perpendicular to the reaction plane depends on $\mathbf{p}_2$ and was calculated according to equations given by Hagedorn.[19] The c.m. pion angle and momentum resulting from this collision were taken as the appropriate kinematical and dynamical parameters for calculating the

corresponding $pp \rightarrow d\pi^+$ differential cross sections for the two spin orientations. This choice of parameters is clearly not unique, and other possibilities, for example the total c.m. energy and the four-momentum transfer, could also be employed. Investigation of these other possibilities was indeed carried out but produced considerably less satisfactory results overall. It was found, furthermore, that the appropriate variable for selecting the energy at which the total NN pion production cross section was calculated was the incident proton c.m. momentum (in the c.m. of the two colliding nucleons). Use of the total c.m. energy (in the c.m. of the two colliding nucleons) or the above pion momentum resulted in considerably lower equivalent energies and hence lower NN pion production cross sections. Thus the angular dependence of the differential cross sections and analyzing powers was defined by the c.m. pion angle and momentum, while the normalization of the spin-dependent differential cross sections via the total cross section was defined by the incident proton c.m. momentum.

Final $NN\pi^+$ states consisting of unbound nucleons were handled approximately by assigning an effective mass to the NN system. This effective mass was the total internal energy of the NN system when the pion had its mean kinetic energy in the $pp \rightarrow pn\pi^+$ reaction.[17] These effective masses were 15—40 MeV greater than the deuteron rest mass, depending on pion angle and proton bombarding energy.

The angular and spin dependence of the $pp \rightarrow d\pi^+$ reaction was taken from Jones.[10] As noted earlier, this same dependence was also assumed for the other $NN \rightarrow NN\pi^+$ reactions. Momentum distributions for p- and s-shell protons in ^{12}C have been measured in (e,e'p) experiments extending to momenta of 300 MeV/c.[18] These were normalized as follows:

$$\int_0^\infty |\phi(p)|^2 p^2 dp = 4.0, \quad p \text{ shell}$$
$$= 2.0, \quad s \text{ shell},$$

corresponding to the shell model limits for the occupancy of the p and s shells. Numerical integration over these momentum distributions was incorporated in the calculations, which were carried out separately for the p- and s-shell protons. In turn, each of these calculations was repeated for the two cases of bound and unbound nucleons in the $NN \rightarrow N\pi^+$ simulated reactions.

Results of these calculations are shown by the solid curves in Figs. 3 and 4. Each of the cross section curves has been separately normalized to the experimental data as shown, with the calculated results multiplied by the factor indicated on each curve. The analyzing power data, on the other hand, is shown with its absolute normalization as given by the calculation. A comparison of the results of this model with the data as displayed in Figs. 3 and 4 indicates that the magnitude and energy dependence of the analyzing powers at forward angles is quite well predicted. At the larger angles the magnitude of the experimental analyzing powers is considerably larger than predicted by this model, although the model predictions are reasonably close to the measured analyzing powers of the $pp \rightarrow d\pi^+$ reaction. Secondly, the cross section calculations in most cases exhibit the general shape of an inverted parabola, consistent with the trend of the data. The maxima of these parabola occur at pion energies close to the pion energy in the free $pp \rightarrow d\pi^+$ reaction, which in turn coincide quite well with the peak of the experimental differential cross sections.

The normalization factors, which are in the neighborhood of 0.8%, should not be taken too seriously since important distortion effects have been ignored, and the calculations reflect a particular choice of kinematical parameters for calculating the total NN pion production cross sections. Other choices, for example using the total c.m. energy of the colliding nucleons, resulted in predicted cross sections only 45% as large. Nevertheless, the consistency of these factors indicates that all these neglected effects, taken collectively, are relatively constant.

The importance of the $pp \rightarrow pn\pi^+$ channel can be judged from its contribution to the total inclusive cross section. In all cases this contribution was greater than that of the $pp \rightarrow d\pi^+$ reaction by 20—50%. The reason for this is to be found in the rapidly increasing cross section for the former process above 480 MeV bombarding energy. The momentum distribution of the struck nucleons results in frequent interactions occurring at equivalent energies considerably above that of the incident proton energy. Since the total $pN \rightarrow NN\pi^+$ cross section is 20% and 50% greater than the $pp \rightarrow d\pi^+$ cross section at about 500 and 536 MeV bombarding energy, respectively, the effective c.m. energies of the NN collisions occur at 2112—2128 MeV, some 50 MeV below the peak of the $N\Delta$ systems.

V. DISCUSSION AND CONCLUSIONS

Inclusive measurements of the differential cross sections and analyzing powers of the (p,π^+) reaction on ^{12}C have been performed at 400 and 450 MeV proton bombarding energy. The cross section, at most of the angles investigated, exhibits a maximum as a function of energy in the neighborhood of the pion energy from the $pp \rightarrow d\pi^+$ reaction. The value of the cross section at this peak is approximately 10 μb sr^{-1} MeV^{-1} at 400 MeV and 13 μb sr^{-1} MeV^{-1} at 450 MeV, and is not strongly dependent on angle. The analyzing powers exhibit a strong energy dependence at forward angles, which is quantitatively reproduced by a quasifree model. Again at forward angles, for pion energies corresponding to the peaks of the cross section distributions, the analyzing powers are very close to those observed in the $pp \rightarrow d\pi^+$ reaction. At larger angles the magnitude of the measured analyzing powers exceeds both the calculated values and the values in the $pp \rightarrow d\pi^+$ reaction by a factor of about 2.

The quasifree model presented in this paper used as input the free NN pion production total cross section data, the free $pp \rightarrow d\pi^+$ differential cross section and analyzing power data, and the measured momentum distributions of protons in ^{12}C. In spite of the crude nature of the model, good overall agreement is obtained in the shape and magnitude of the differential cross sections, and the energy dependence of the analyzing powers. These observations provide strong evidence for the interpretation of the in-

clusive pion production mechanism in terms of primary $NN \rightarrow NN\pi^+$ quasifree reactions. More extensive measurements over a wide range of angles and energies, together with coincidence measurements between the pion and deuteron (or other particles), would do much to enhance our understanding of inclusive nuclear pion production mechanisms.

ACKNOWLEDGMENTS

The extensive assistance of D. Sample in the data analysis is gratefully acknowledged. This work was supported in part by the Natural Sciences and Engineering Research Council of Canada.

---

*Present address: Department of Physics and Astronomy, University of Regina, Regina, Saskatchewan, Canada.

[1]J. F. Crawford, M. Daum, G. H. Eaton, R. Frosch, H. Hirschmann, R. Horisberger, J. W. McCulloch, E. Steiner, R. Hausmammann, R. Hess, and D. Werren, Phys. Rev. C **22**, 1184 (1980).

[2]L. Bimbot *et al.*, Nucl. Phys. **A440**, 636 (1985).

[3]N. J. DiGiacomo *et al.*, Phys. Rev. C **31**, 292 (1985).

[4]E. L. Mathie, Ph.D. thesis, University of British Columbia, 1980 (unpublished).

[5]D. Beder and P. Bendix, Nucl. Phys. **B26**, 597 (1971).

[6]M. M. Sternheim and R. R. Silbar, Phys. Rev. D **6**, 3117 (1972); R. R. Silbar and M. M. Sternheim, Phys. Rev. C **8**, 492 (1973).

[7]Z. Fraenkel *et al.*, Phys. Rev. C **26**, 1618 (1982), and references contained therein.

[8]W. A. Ziegler, M.Sc. thesis, University of British Columbia, 1983 (unpublished).

[9]C. Richard-Serre, W. Hirt, D. F. Measday, E. G. Michaelis, M. J. M. Saltmarsh, and P. Skarek, Nucl. Phys. **B20**, 413 (1970).

[10]G. Jones, in *Pion Production and Absorption in Nuclei—1981 (Indiana University Cyclotron Facility),* Proceedings of the Conference on Pion Production and Absorption in Nuclei, AIP Conf. Proc. 79, edited by Robert D. Bent (AIP, New York, 1982), p. 15.

[11]B. J. Ver West and R. A. Arndt, Phys. Rev. C **25**, 1979 (1982).

[12]G. Giles, Ph.D. thesis, University of British Columbia, 1984 (unpublished); and to be published.

[13]D. V. Bugg, J. A. Edgington, C. Amsler, R. C. Brown, C. J. Oram, K. Shakarchi, N. M. Stewart, G. A. Ludgate, A. S. Clough, D. Axen, S. Jaccard, and J. Varra, J. Phys. G **4**, 1025 (1978).

[14]*Polarization Phenomena in Nuclear Reactions,* edited by H. H. Barschall and W. Haeberli (University of Wisconsin Press, Madison, Wisconsin, 1970), p. xxv.

[15]W. R. Falk *et al.*, TRIUMF Report TRI-PP-83-127, 1983.

[16]W. R. Falk, E. G. Auld, G. Giles, G. Jones, G. J. Lolos, P. Walden, and W. Ziegler, Phys. Rev. C **25**, 2104 (1982).

[17]W. R. Falk *et al.*, Phys. Rev. C **32**, 1972 (1985).

[18]J. Mougey, Nucl. Phys. **A335**, 35 (1980); J. Mougey, Commissariat à l'Energie Atomique Internal Report, 1975.

[19]R. Hagedorn, *Relativistic Mechanics* (Benjamin/Cummings, Reading, Mass., 1963), p. 124.